



Artificial neural networks in the application of the growth of the urban sprawl Redes neuronales artificiales en la aplicación del crecimiento de la mancha urbana

E. Jiménez-López ^{a,*}, L. A. López-Rivero ^b

^a El Colegio Mexiquense A.C., 51350, Zinacantepec, Estado de México, México.

^b Facultad de Ingeniería, Universidad Autónoma del Estado de México, 50100, Toluca, Estado de México, México.

Abstract

The objective of this work is the use of artificial neural networks and cellular automata to support urban planning decisions in Mexico. We propose an automated model that predicts vertical urban growth, using socio-economic and geographic factors. A multidisciplinary model is presented, which uses artificial neural networks, cellular automata, spatial analysis methods and image processing. The model allows different scenarios of urban growth to be projected and simulated. All of this is built into QGIS through the Python programming language. The model is tested in Mexican cities such as Mexico City, Guadalajara and Monterrey during 2015 to 2020. Reliability ranges from 72% to 76% were obtained and validated by: i) the average number of projected skyscrapers, ii) Position using the Kappa index, and iii) Value in the image using the Jaccard index. With this we propose a technique that allows better informed decisions for urban planning and anticipate new infrastructure needs, projections and regulations.

Keywords: Artificial neural network, Cellular automata, Vertical urban growth.

Resumen

El objetivo de este trabajo es el uso de redes neuronales artificiales y autómatas celulares que apoyen las decisiones de planeación urbana en México. Proponemos un modelo automatizado que predice el crecimiento urbano vertical, utilizando factores socioeconómicos y geográficos. Se presenta un modelo multidisciplinario que maneja redes neuronales artificiales, autómatas celulares, métodos de análisis espacial, y procesamiento de imágenes, que permiten proyectar y simular diferentes escenarios de crecimiento urbano. Todo esto está integrado en QGIS a través del lenguaje de programación Python. El modelo se prueba en ciudades mexicanas como Ciudad de México, Guadalajara y Monterrey durante los años 2015 a 2020. Se obtuvieron rangos de confiabilidad de 72% a 76%, validados por: i) el número promedio de rascacielos proyectados, ii) Posición usando el índice Kappa, y iii) Valor en la imagen usando el índice Jaccard. Con esto proponemos una técnica que permite tomar decisiones mejor informadas para la planificación urbana y anticipar nuevas necesidades de infraestructura, proyecciones y normativas.

Palabras Clave: Redes Neuronales Artificiales, Autómatas Celulares, Crecimiento urbano vertical.

1. Introduction

Artificial Neural Networks (ANN) is an analogy of the biological neural network that behaves as a processing element. This processing element takes multiple inputs and combines them, usually with a basic sum. The sum of the inputs is modified by a transfer function and the value of the output is passed directly to the input of another set of nodes

through weighted connections corresponding to a given task (Rajasekaran and Pai, 2003).

The interest in developing ANN's lies not only in the processing model but also in the ways in which these processing elements are connected. Network nodes are generally organized into groups called levels or layers. A typical network consists of a sequence of layers with connections between consecutive adjacent layers. There are two layers with connections to the outside world. An input

*Autor para la correspondencia: ejimenez@cmq.edu.mx

Correo electrónico: ejimenez@cmq.edu.mx (Eduardo Jiménez-López), lrluyz@gmail.com (Luis Antonio López-Rivera).

Historial del manuscrito: recibido el 15/02/2023, última versión-revisada recibida el 22/05/2023, aceptado el 23/05/2023, en línea (postprint) desde el 25/05/2023, publicado el 05/07/2023. **DOI:** <https://doi.org/10.29057/icbi.v11i21.10565>



layer, where data is presented to the network, and an output buffer layer, which contains the network's response to an input. The rest of the layers are called hidden layers (Agatonovic-Kustrin and Beresford, 2000).

The ANN generates its own learning rules from the examples shown in the training phase, the network becomes an expert system due to the experience it acquires when connecting. The processing power of the ANNs is mainly measured by the number of interconnections updated per second during the training or learning process. Learning is achieved through a learning rule that adapts or changes connection weights in response to input instances, and also in response to desired outputs. This feature of ANNs is what allows us to say that neural networks learn from experience. An important characteristic of ANNs is the form or manner in which the information is stored. The memory or knowledge of these networks is distributed among all the weighted connections of the network. On partial input, the network, will house the most similar connection path in memory and generate an output that corresponds to the full input (Bose, 1994). The partial input in some artificial neural networks has the characteristic of being "associative" which means that the network will choose the most similar input in memory and generate an output that corresponds to the complete input.

Currently, technological developments in geography have begun to integrate techniques such as ANN into urban growth models to simulate the behavior of cities or regions, considering human and geographic factors (Silva, 2004). This type of model presents an area of opportunity that is growing because they simulate the behavior of the human brain (Wu and Silva, 2010).

Urban growth is seen as a spatial-temporal phenomenon that arises because of social, economic or geographic factors and occurs both horizontally and vertically (Zhang *et al.*, 2018). Urban growth does not occur randomly, but results from actions that drive urban growth called driving forces or factors that are considered as proximity to public services, accessibility to resources, population density, location of industrial zones, economic dependency, among others. Urban expansion generates environmental and social consequences, such as the destruction of forests, agricultural areas and spaces destined for water reserves (Koziatek and Dragičević, 2019). In addition to the increasingly long journeys to daily activities, impacting the time required to access services. The creation of new human settlements in the peripheries increases public spending, affecting the economy, so it is considered that vertical urban growth can reduce these actions (Zhao *et al.*, 2017).

City developers opting for vertical growth have adapted by creating ever taller buildings and using them as tools to integrate services and reduce damage to natural areas (Agyemang *et al.*, 2018; Parker, 2014). Opting for vertical growth has some theoretical benefits reported in the literature, for example: i) Sustainable planning that aims to generate savings in the construction of public infrastructure (Shim *et al.*, 2004), ii) Shorter travel distances between residences and places of work, reducing traffic caused by dependency on commuting (Mualam *et al.*, 2019), iii) Multipurpose buildings, combining residential, office and commercial facilities, with different functions 24 hours a day (Shim *et al.*, 2004) and iv) Increase in sustainable energies, since roofs can be covered with solar panels or agricultural spaces (Huang *et al.*, 2019).

The development of this work links the vertical growth generated by ANN to Geographic Information Systems (GIS), which is one of the most used tools by city developers. Therefore, a vertical growth model fully integrated with free software GIS is presented, programmed in Python from scratch to have the certainty of the deep knowledge generated by the neural network. This development estimates not only the number of future skyscrapers but also the areas that are most likely to host new skyscraper developments in the future, all of this generated by the connections and weights in the nodes of the network that are factors that favors growth, portrait of the city. Models and simulations are usually used to understand, test and experiment with social theories regarding complex processes as vertical grown. Using modelling and simulation, different plans are studied and possible scenarios are examined in advance to evaluate different policies and strategies regarding urban management (Kaviari *et al.*, 2019).

2. Study area and data

We use raster images from the Landsat 8 satellite and georeferenced data on population, housing, economically active population and services factors from the Mexican Institute (INEGI) for the period 2015 – 2020, skyscrapers are selected from (SKYCPAPER, 2020; EMPORIS, 2020) databases according to the Council on Tall Buildings and Urban Habitat (CTBUH, 2020), which considers skyscraper as a building that is at least 20 floors or 100 meters high. The model is tested with the three most important metropolitan areas in Mexico: a) Mexico City, b) Guadalajara and c) Monterrey.

Vertical growth in Mexico City, as depict in Figure 1(a), is the largest and most populated area in Mexico with a total of 25,916,842 inhabitants and an area of 7,854 Km². The City of Guadalajara (Figure 1(b)), is the second most populated region in México with a total of 4,887,383 inhabitants (INEGI, 2015a). Finally the city of Monterrey (Figure 1(c)), has a very high population growth rates exceeding10%. Table 1 summarizes the working data.

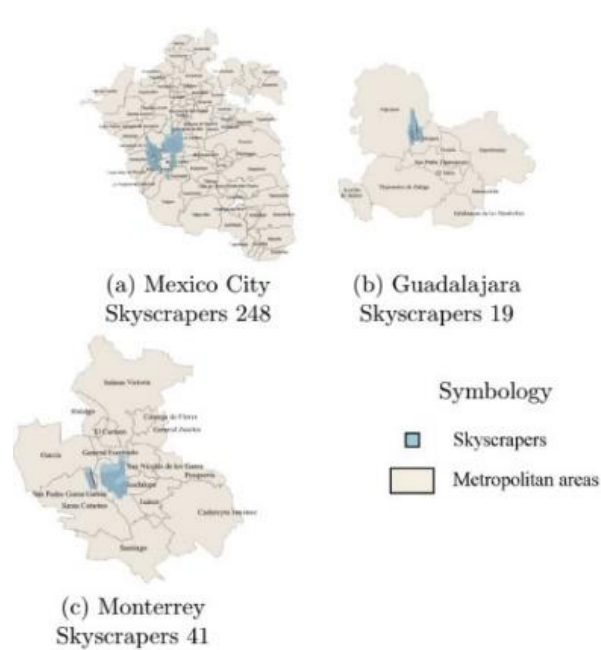


Figure 1: Metropolitan study areas.

Vertical growth in Mexican cities is due to the economic, technological and social importance of metropolitan areas (Zhao *et al.*, 2017). Where the metropolitan area is the territory that includes the nearby municipalities of a large city and a set of populations around it, in which joint planning actions are developed. The lack of government support and poor urban planning result in vertical areas far from workplaces or not very useful (Felix, 2015).

In previous research such as (Zhao *et al.*, 2017; Felix, 2015) highlight the importance of driving factors such as population, economy, housing, land type and access to services, the data of these factors are considered in the proposed model of this work for simulating vertical growth scenarios, and these factors are described in Table 1.

coordinating, collecting and disseminating information on Mexico in terms of territory, resources, population and economy (INEGI, 2015b).

3.1.1. Raster images

Three sets of satellite images are downloaded for the metropolitan areas, where each set contains two images, one for the year 2015 and one for the year 2020. For each satellite image, a pre-processing is carried out to reduce noise, distortion or alteration errors of values produced at the time of capture (Irons *et al.*, 2012) in accordance with the homogeneity in the methodologies proposed by (Bhatti *et al.*, 2014; Burton-Johnson *et al.*, 2016).

After that, we apply the semi-automated pan-sharpening methods proposed by (Gomez *et al.*, 2013; ESRI, 2016), this increases the resolution in the satellite bands improving the

Table 1: Working dataset used.

Data	Description	Data Type	Source
Study area	Vectorial maps of metropolitan areas	Polygon (.shp)	INEGI (2019).
Landsat images	Landsat images of metropolitan areas	Raster (.tif)	USGS (2020).
Skyscrapers	Points with coordinates of buildings	Points (.shp)	(SKYCPAPER, 2020; USGS, 2020).
Population	File with data population factor	Polygon (.shp)	INEGI (2015b).
Population (EAP)	File with data EAP factor	Polygon (.shp)	INEGI (2015a).
Housing	File with data housing factor	Polygon (.shp)	INEGI (2015c).
Services	File with data services factor	Polygon (.shp)	INAFED (2015).

Table 2: indices interpretation for urban area extraction

Data	Purpose	Equation	Interpretation (I)
NDVI (V)	Is used for the extraction of vegetation	$V = \frac{B4 - B3}{B4 + B3}$	$I = \begin{cases} \text{Water or snow } I < 0 \\ \text{No vegetation } 0 \leq I < 0.1 \\ \text{Rocked } 0.1 \leq I \leq 0.2 \\ \text{Bush } 0.2 \leq I \leq 0.3 \\ \text{Vegetation } I > 0.3 \end{cases}$
MNDWI (W)	Remove water signatures and increase the spectral contrast among built-up area	$W = \frac{B3 - B7}{B3 + B7}$	$I = \begin{cases} \text{No vegetation or water } I < 0 \\ \text{Vegetation or water } I \geq 0 \end{cases}$
NDBI (B)	Useful for mapping urban built-up areas	$B = \frac{B6 - B5}{B6 + B5}$	$I = \begin{cases} \text{Vegetation } I < 0 \\ \text{Crops } 0 < I < 0.5 \\ \text{Building area } I > 0.5 \end{cases}$
BAEM (U)	Built-up area free of noise, water bodies and vegetation	$U = V - W - B$	$I = \begin{cases} \text{No build up area } I < 127 \\ \text{Build up area } I \geq 127 \end{cases}$

3. Modelling

The proposed model in this research, presented in Figure 2 has four main parts: i) Study area data processing, ii) ANN architecture search, iii) Vertical growth projection using Cellular Automata (CA) and iv) Validation of results.

3.1. Data Processing

The variables shown in Table 2 are the combination of the spectral bands in the satellite image, we use two data types, raster images and vector data of 2015 and 2020. The former come from the Landsat 8 satellite, while the latter are provided by INEGI, which is a public body responsible for regulating,

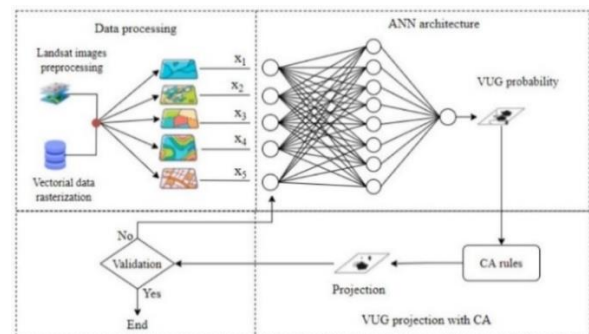


Figure 2: Vertical urban growth proposed model

Visualization and interpretation of the images (Sabater *et al.*, 2016). In order to highlight the built-up area in resulting images, we classified different land types such as: snow, vegetation, water, crop fields, among others (Bhatti *et al.*, 2014).

The classification method extracts the built-up area BAEM through integration of three indexes: normalized difference vegetation NDVI, normalized difference water MNDWI and normalized difference built-up NDBI, presented in Table 2.

Finally, the pixels values x_{ij} from each BAEM images are normalized in a value between 0 and 1, considering the maximum "*max*" and minimum "*min*" value in each image according to the following:

$$z_{ij} = \frac{x_{ij} - \min}{\max - \min} \quad (1)$$

Data normalization means bringing each pixel to a standard scale without causing any significant distortion (Kotkar and Jadhav, 2015). Normalized values treat them as equally important inputs to ANN and makes them compatible with the activation functions (Richardson and Van Oosterom, 2002, results are shown in Figure 3.

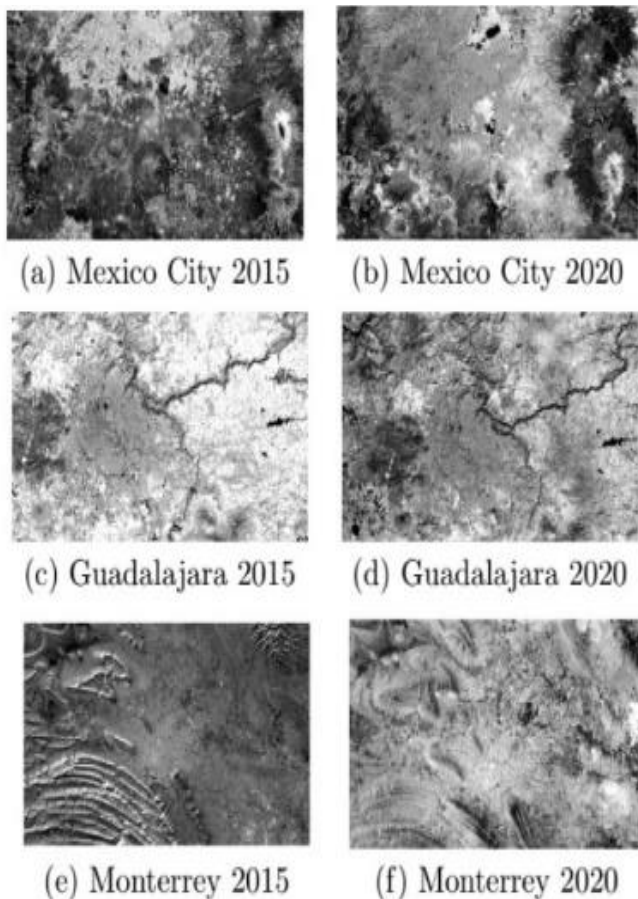


Figure 3: Standardized images of metropolitan areas.

3.2. Vectorial data

Analysis with ANN on vertical growth has found that determining factors such as land price, land type, population density, economic factors, accessibility to transportation services, industrial facilities, schools, hospitals and public safety combined with good residential location trigger an

increase in vertical growth of buildings (Zhao *et al.*, 2017; Abhishek *et al.*, 2017; Mustafa *et al.*, 2017).

In this work, the population, housing, economically active population and services factors are considered, they are downloaded in *.xlsx* files for the projection of vertical growth. the methodology that we follow is the following i) georeferenced according to their metropolitan area. ii) vector files are rasterized using the QGIS Rasterize tool (EMPORIS, 2020), which allows standardizing the *.tif* working data type for later use in the ANN and AC. iii) the resulting images are normalized using the Equation 1.

The rasterization process produces a total of twelve images, four for each study area, where values close to 1 (white) represent a higher amount of population, housing or services and values close to 0 (black) represent the opposite, Figure 4 shows four examples.

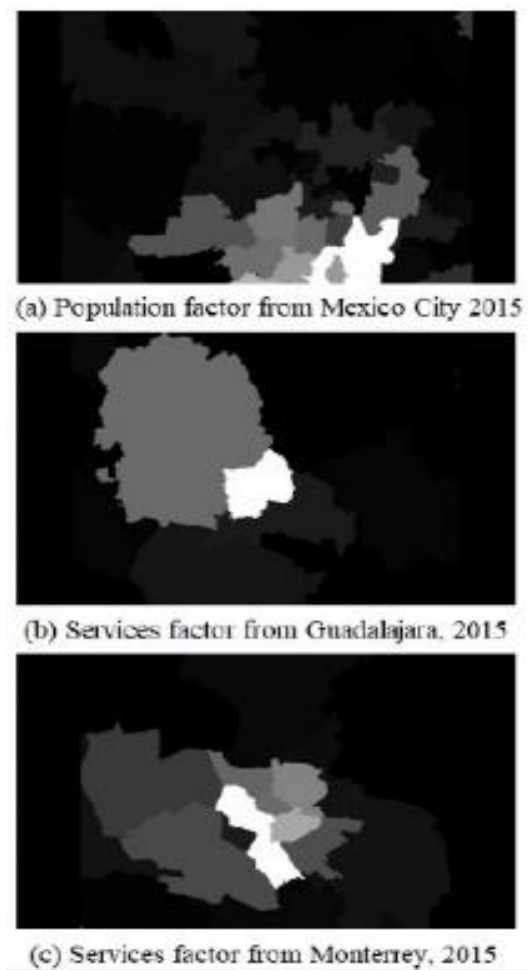


Figure 4: Raster and scaled factors examples, where values close to 1 (white) represent a higher value.

4. Artificial neural network architecture

An artificial neural network is an artificial intelligence technique (Haykin and Network, 2004) that aims to model the learning process of the human brain using electrical components or software programs (Kristollari and Karathanassi, 2020).

The mathematical model of neuron shown in Figure 5 serves as the basis for the process consisting of a vector inputs x_1, \dots, x_D and synaptic weights w_1, \dots, w_D whose single output

y is calculated by applying a weighted sum of inputs and weights $\sum_{i=1}^D w_i x_i + w_0$ and an activation function g .

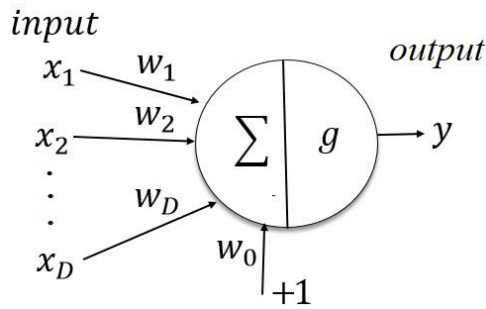


Figure 5: Neuron model based on (Palma and Morales, 2008).

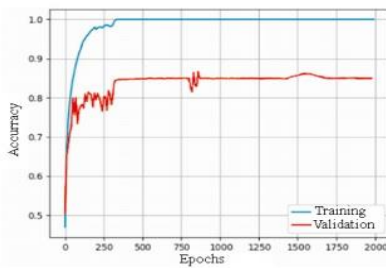
days, testing a total of 501 architectures with 500 training epochs for each metropolitan area.

Once the best architecture for each study area has been selected, it is trained again for 2000 epochs, the results are shown in Table 3, for each city that has been studied so far the results are different. The explanation of the notation is as follows for the values (5,10,13), it should be interpreted as an architecture consisting of three hidden layers, with five neurons in the first layer, ten in the second layer and thirteen in the third layer.

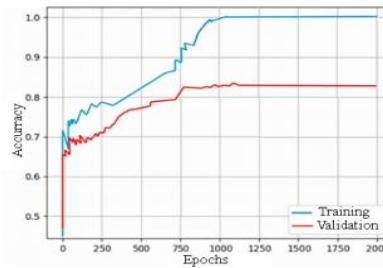
The contrast in the evolution of the learning process during the training and validation stage for each neural network architecture is shown in Figure 6. It is observed that for the three study areas the network reaches its maximum accuracy value in the first 1000 epochs.

Table 3: ANN architecture results for metropolitan areas.

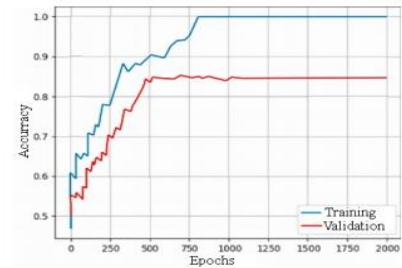
Variable	Mexico City	Guadalajara	Monterrey
Hidden layers	3	4	3
Nodes in hidden layers	(5, 10, 13)	(5, 8, 10, 12)	(5, 13, 14)
Hidden layers activation	Rectified Linear Unit	Hyperbolic tangent	Rectified Linear Unit
Output layer activation	Sigmoid	Sigmoid	Sigmoid
Accuracy	85.47%	86.32%	84.77%



(a) Mexico City



(b) Guadalajara



(c) Monterrey

Figure 6: Training and validation results for metropolitan areas.

Model, it is the combination of various layers and neurons, the connection between them and the type of hardware and software, which makes ANN a tool capable of adapting to solve different kinds of problems (De Sa, 2012).

Even though, the literature considers that there is no universal optimal structure for all applications (Wang *et al.*, 2015), determining the type of ANN and then its architecture is often the best design choice (Ou *et al.*, 2018). Thus, we develop a module for searching the ANN architecture implemented in Python with the Tensorflow and Keras libraries. It proves several ANN architectures by varying the parameters of hidden layers, neurons in hidden layers, hidden layer activation function, activation function in output layer and optimization until a loss of less than 25% is obtained in the architecture.

Each investigation presents a different network architecture, resulting in ANN's being determined by the number of layers, neurons, and type of network to implement (Almeida *et al.*, 2008). This module has been run on a computer with an Intel Core i7 3.1GHz processor, 16GB RAM, Windows 10 64-bit operating system, for a period of 17

4.1. Cellular Automata Rules

Cellular automata is a mathematical model which can be defined by the tuple (d, S, H, δ) where d represents the n -dimensional space, S the states set, H the neighbourhood space and δ the transition rules (Jiménez *et al.*, 2018). A set of five conditions: a) There is a divided space in the form of networks or arrays, b) There are discrete time and discrete states, c) Each cell takes a finite number of states and is updated, according to the states of its neighbors, d) each cell neighborhood is uniformly defined, and e) cells update their state by applying the same transition rules (Adamatzky, 2018).

We propose four factors that converge in a transition rule for vertical growth projection based on two of the main geographic theories: i) the modifiable unit area problem (Openshaw and Taylor, 1984) and ii) the first law of geography of Tobler (Tobler, 1970), and considering a four-level neighborhood system in the sample skyscrapers.

4.1.1. Factor 1: Land use parameter

Through an expert-supervised classification we identified intervals of the land type to which each pixel belongs in the satellite images of the study areas, and the pixels where a

skyscraper is based in the raster images. Results are shown in Table 4, where the $(a, b]$ notation stands for a half-closed interval and $[a, b]$ notation stands for a closed interval.

similarly tv_i a list with the form $tv_i = [v_0, v_1, v_2, v_3, v_4]$ where each v_i represents a risk level assigned in Table 5. The risk parameter r is calculated by the weighted sum between the

Table 4: Land type classification ranges.

Land use	Mexico City	Guadalajara	Monterrey
Water	[0.00, 0.31]	[0.00, 0.23]	[0.00, 0.29]
Construction land	(0.31, 0.52]	(0.23, 0.30]	(0.29, 0.43]
Roads-Highways	(0.52, 0.58]	(0.30, 0.38]	(0.43, 0.48]
Build-up area	(0.58, 0.67]	(0.38, 0.54]	(0.57, 0.61]
Green spaces	(0.67, 1.00]	(0.54, 1.00]	(0.61, 1.00]
Skyscrapers	[0.53, 0.63]	[0.25, 0.35]	[0.39, 0.57]

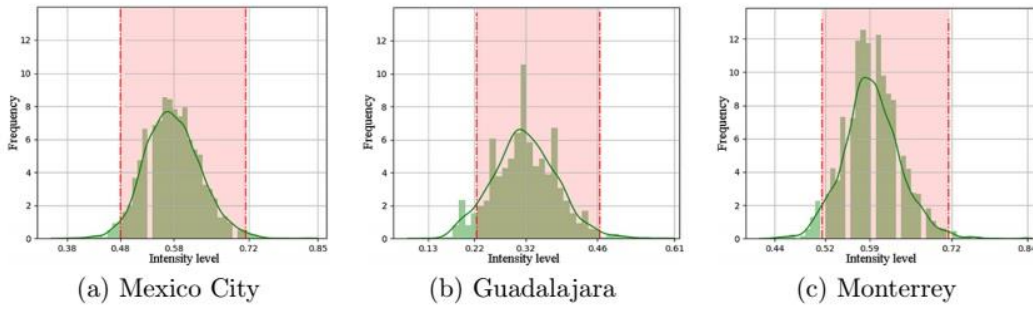


Figure 7: confidence intervals calculated for the study areas.

The use of intervals in the CA throws up a restrictive rule that prohibits the construction of vertical developments on land identified as water, roads-highways and green spaces, which are often not respected in horizontal growth (He *et al.*, 2017; Duque *et al.*, 2019).

4.1.2. Factor 2: Confidence interval parameter

The calculation of the confidence intervals provides an interval within the value that would be expected for each parameter in question (Montgomery, 2017). Therefore, this rule ensures, at a confidence level, that vertical growth occurs in areas with characteristics similar to the neighborhood space in the sample skyscrapers.

For this purpose, goodness-of-fit tests are carried out using the Kolmogorov-Smirnov (Massey, 1951), Anderson-Darling (Anderson and Darling, 1954) and Chi-square (Tallarida and Murray, 1987), calculations included in the Scipy Python library. The calculation identifies Beta and Normal distributions as optimal for calculating intervals using:

$$\bar{y} - Z_{\frac{\alpha}{2}} * \frac{\sigma}{\sqrt{n}} \leq \mu \leq \bar{y} + Z_{\frac{\alpha}{2}} * \frac{\sigma}{\sqrt{n}} \quad (2)$$

The 95% confidence intervals were calculated and shown with a red shaded in the graphs of Figure 7.

4.1.3. Factor 3: Risk parameter

It is designed taking into account the firmness and land uses defined by the INEGI soil science service (INEGI, 2020), whose objective is to identify how much risk exists in the neighborhood of skyscrapers, and if this is higher than the estimated threshold, the growth vertical is limited.

Letting tp_i be a list of the form $tp_i = [u_0, u_1, u_2, u_3, u_4]$ where each element u_i represents the total number of pixels in the satellite image for each land use defined in Table 5,

elements of tp_i and tv_i , divided by the total pixels tp of the neighbourhood without considering the central pixel, as follows:

$$r = \frac{\sum_{i=0}^4 tp_i * tv_i}{tp} \quad (3)$$

The application of the risk equation 3 is shown:

$$r = \frac{u_0 * v_0 + u_1 * v_1 + u_2 * v_2 + u_3 * v_3 + u_4 * v_4}{tp} \quad (4)$$

$$r = \frac{0 * 0.2 + 12 * 0.4 + 32 * 0.6 + 36 * 0.8 + 0 * 1}{80}$$

$$r = 0.66$$

The process of applying the rule in the CA consists of: a) locate a central pixel, b) count the pixels of each land type in its neighborhood (Figure 8).

The permissible risk threshold in each metropolitan area is calculated using confidence intervals ($1 - \alpha = 98\%$) in the sample skyscrapers, considering an average between the upper and lower level as the allowable threshold value. The proposed parameter values are presented in Table 5.

4.1.4. Factor 4: Influence area parameter

This parameter determines the density of buildings that exist in the approximate area for a block in Mexico ($500m^2$) and indicates the level of probability that vertical grown occurs from the skyscrapers influence in the area, using the kernel-density estimation (KDE).

Given a data set $n = [x_1, x_2, \dots, x_n]$, the KDE parameter $\hat{f}_h(x)$ estimates the points number that exist within a given area h ; the points influence within the area, and it is associated with a distribution of probability K_h , which decreases as the distance increases and vice versa (Lampe and Hauser, 2011).

$$f_h(x) = \frac{1}{n} \sum_{i=1}^n K_h(x - x_i) \tag{5}$$

In this research a Gaussian kernel from the statistical functions in the Python SciPy module is used. The influence area parameter favors vertical grown in areas with a high, very high and medium building influence, as shown in Figure 9.

To determine the best CA rule, we involve all the previously discussed factors, i.e. analysis of Land use parameter, Confidence interval parameter, Risk parameter and Influence area parameter.

Cellular Automata underlie the dynamics of change events based on the factor proximity concept: the closer to existing areas of the same class the more likely they are to

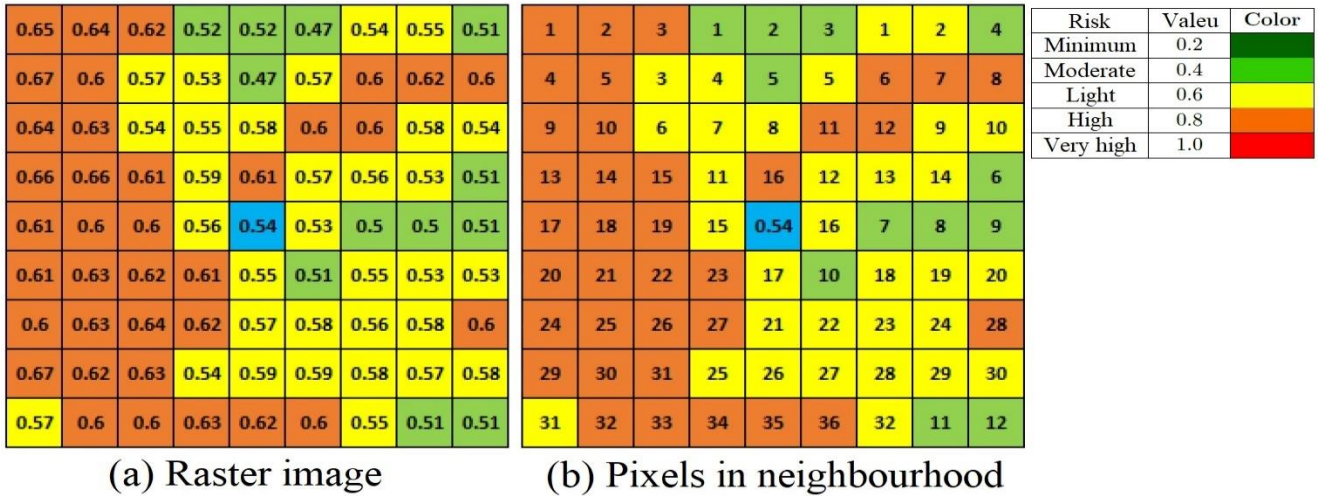


Figure 8: Risk parameter application process in the CA.

Table 5: Proposed risk values for the cellular automaton rule.

Land use	Mexico City	Guadalajara	Monterrey
Water	[0.00, 0.31]	[0.00, 0.23]	[0.00, 0.29]
Construction land	(0.31, 0.52]	(0.23, 0.30]	(0.29, 0.43]
Roads-Highways	(0.52, 0.58]	(0.30, 0.38]	(0.43, 0.48]
Build-up area	(0.58, 0.67]	(0.38, 0.54]	(0.57, 0.61]
Green spaces	(0.67, 1.00]	(0.54, 1.00]	(0.61, 1.00]
Skyscrapers	[0.53, 0.63]	[0.25, 0.35]	[0.39, 0.57]

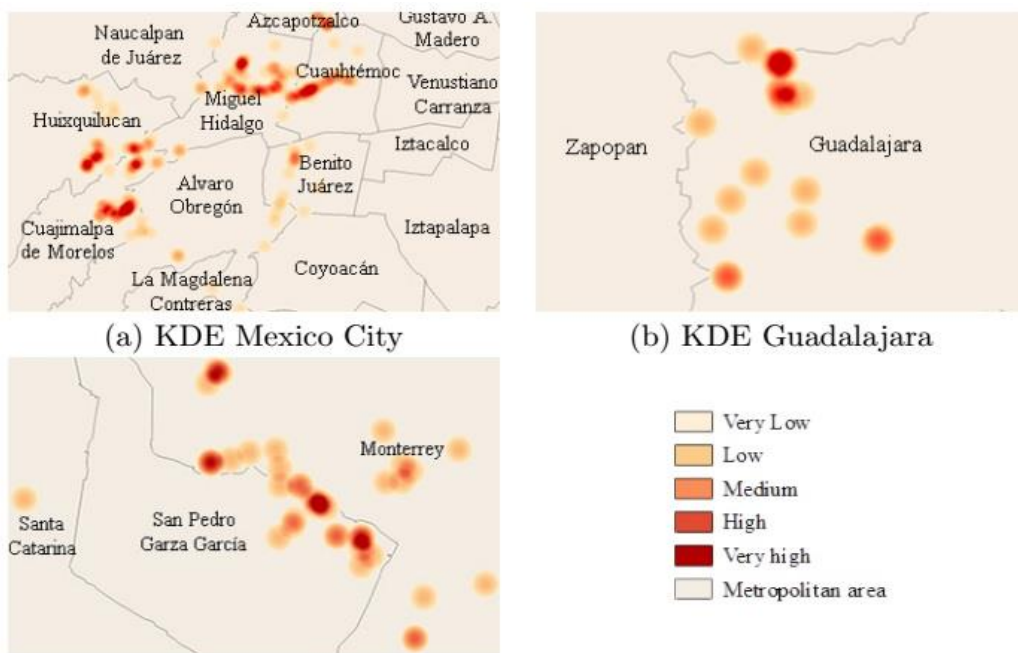


Figure 9: Influence parameter in metropolitan areas.

change to a different class. A cellular automaton is a cellular entity that varies its condition based on its previous state (according to factors included in vertical growth) and adjacent neighbors. In this work a contiguous filter rule of 5x5 cells is used as shown in Figure 10.

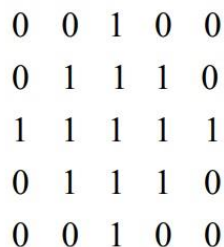


Figure 10: Proximity rule in vertical growth.

5. Validation

Using data from 2015, years 2020 and 2025 are projected, the projected number of buildings is contrasted with real data and their position is compared using the Kappa index k for results validation, where P_0 is the observed equality, P_e is the expected equality and $(1 - P_e)$ represents the maximum equality or concordance (Jiménez, 2022).

$$k = \frac{P_0 - P_e}{1 - P_e} \tag{6}$$

Furthermore, the similarity between maps in different periods of time is evaluated using the Jaccard index J , where T_{21} are the image A elements, T_{12} image B elements and T_{11} A with B junction elements (Bouchard *et al.*, 2013; Jiménez, 2022).

$$J = \frac{T_{11}}{T_{21} + T_{12} + T_{11}} \tag{7}$$

In Table 6, we use an interpretation based on the proposal of (Jiménez, 2019) that works with satellite images for the interpretation of the k and J indexes.

Table 6: Kappa and Jaccard indexes evaluation and interpretation.

Value	Equality level	
	Kappa index	Jaccard index
≤ 0.0	Not equality	-----
(0.0, 0.2]	Insignificant	Insignificant
(0.2, 0.4]	Low	Low
(0.4, 0.6]	Moderate	Moderate
(0.6, 0.8]	Good	Good
(0.8, 1.0]	Total equality	Total equality

6. Results

The 2015-2020 projection in terms of the number of buildings has an average precision of 75.81%, with a Kappa index of 0.7317 and a Jaccard index of 0.7606 (Table 7), which is a good estimate, based on the Table 6. In addition, the 2020-2025 projection estimates a vertical growth rate of 15.63% (Figure 11).

Geographically speaking, the model projects a vertical growing in the Santa Fe area (Mexico City), we believe that is

not only because the concentration of buildings, but also because of the population and economy factors are higher in comparison to other areas on that metropolitan area. In addition, this area is likely to grow vertically because most of the buildings are headquarters, also it is located between two of the most important roads in the city: Santa Fe Avenue and Paseo de la Reforma, which increases its accessibility.

On the other hand, the projection to 2025 shows that the vertical growth begins to expand towards the municipalities of Gustavo A. Madero, Iztacalco, Tlalnepantla, Naucalpan, La Magdalena Contreras and Tlalpan in Mexico City, with a total of 339 buildings that exceed 100 meters in height. On the other hand, the municipalities of Huixquilucan and Miguel Hidalgo project vertical growth from 2,020 to 2,025 with 7 and 8 additional skyscrapers, respectively. As shown in Figure 12.

The 2015-2020 projection for the Guadalajara in terms of the number of buildings scores an average accuracy of 75.87%, with a Kappa index of 0.7472 and a Jaccard index of 0.7723 (Table 7), which is a good estimation, according to Table 6. Furthermore, the 2020-2025 projection estimates a vertical growth rate of 13.57% (Figure 11).

The results of Figure 11 show a vertical growth trend towards the center of the municipality of Zapopan., which may be due to its larger distribution of land available for construction and that with respect to (INAFED, 2015) data the total population, housing and EAP is just under 1%, compared to Guadalajara.

The Guadalajara factors in the Zapopan and Guadalajara municipalities are higher than the rest of the municipalities, which increases the probability of vertical growth in those areas, with a skyscraper distribution of 81% and 19% respectively. This concentration has resulted in the Mexican Association of Real Estate FIBRAS (AMEFIBRA), investing in land for commercial, hotel and office buildings in the municipality of Jalisco.

The 2015-2020 projection for the Monterrey in terms of the number of buildings scores an average accuracy of 73.61%, with a Kappa index of 0.6866 and a Jaccard index of 0.7109 (Table 7), which is a good estimation, according to Table 6. Furthermore, the 2020-2025 projection estimates a vertical growth rate of 41.66% (Figure 11).

Vertical growth in the Monterrey is concentrated in 5 of the 18 municipalities that form it, with Monterrey and Garza Garcia being the predominant ones with 93% of the total number of skyscrapers in the area. However, data from (INEGI, 2015b) show an accelerated growth in population and housing in the municipality of Guadalupe, which has increased the real estate market dynamism.

The vertical growth in the Santa Catarina municipality is increasing due to its proximity to Garza Garcia and Monterrey, with four new skyscrapers by 2025, similar to San Nicolas de los Garza with two skyscrapers projected, showing a vertical growth to the north and south of the area.

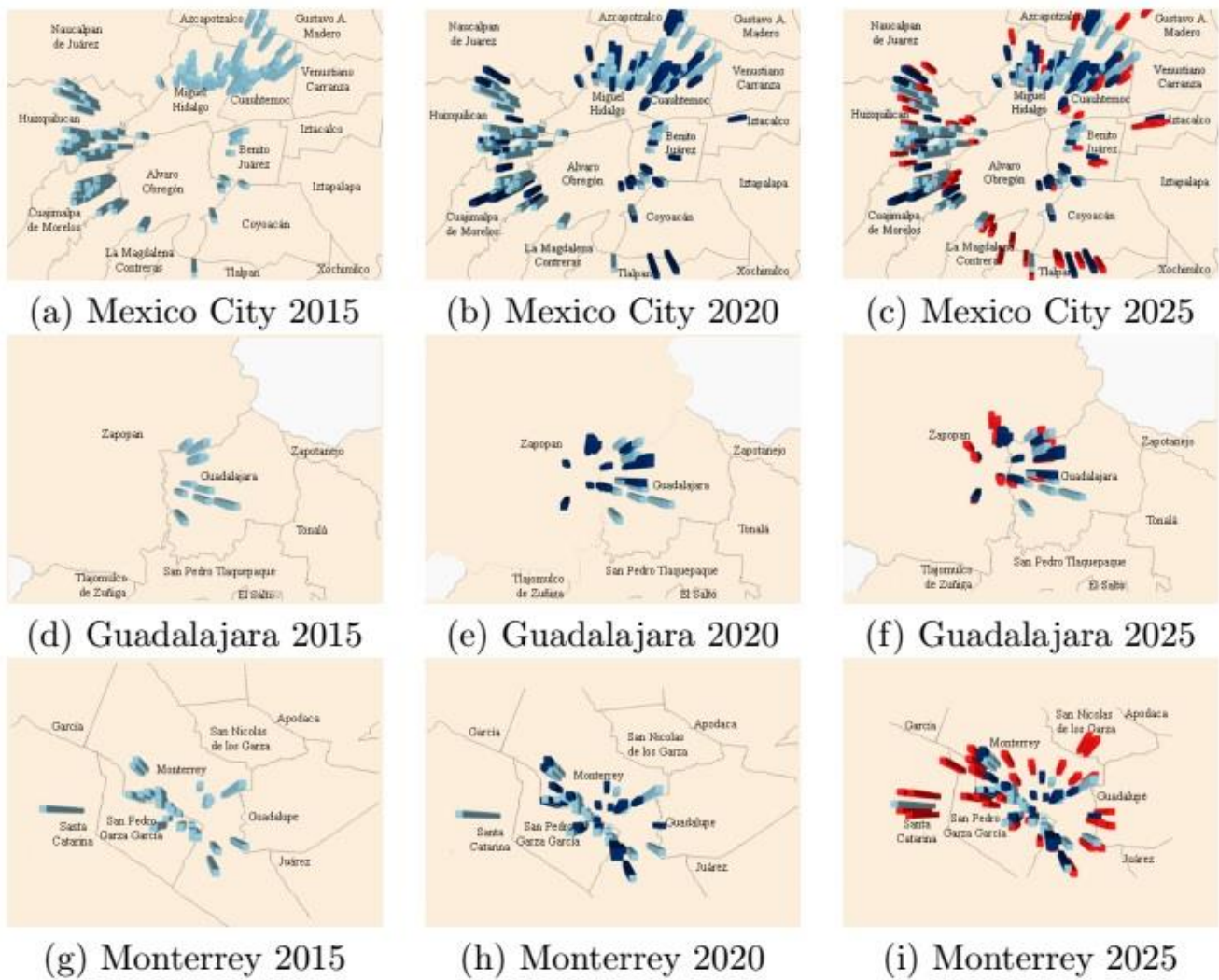


Figure 11: vertical urban growth projections in metropolitan areas.

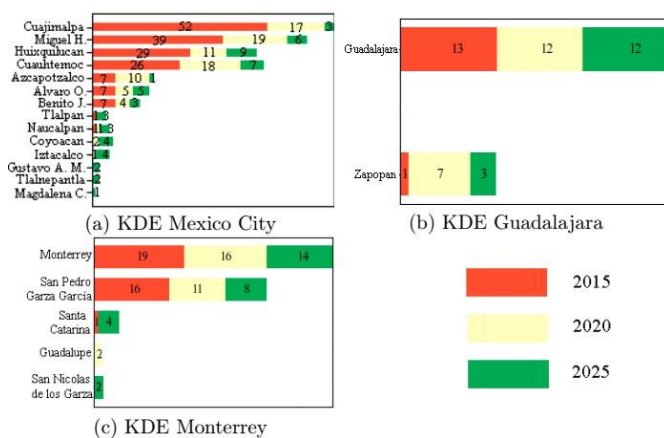


Figure 12: Vertical urban growth by municipality in the metropolitan areas.

7. Conclusions

The ANN has great advantages over other typical models for solving geosimulation problems due to its great ability to learn from experience, generalize problems and not memorize them. The ANN, after being trained and tested, can be applied in real-time systems due to its great parallel processing

capacity, as shown in this work. The number of hidden layers and the number of neurons in this layer is chosen according to the experience of the programmer and is sometimes done by trial and error.

Applications that exploit the characteristics of ANNs and apply it to the field of geosimulation. However, there are still very large limitations. The main problem consists in the proper meeting of georeferenced information and the driving factors of vertical growth. It is important to keep in mind that the ANN is a model of information processing, this system tries to emulate an ideal model that is very close to reality.

The results show that vertical growth in the study areas is centralized and begins to expand gradually, due to the interaction of vertical growth factors. Analyzing the results of various vertical growth scenarios by modifying the driving factors or CA rules, allows better informed decisions for urban planning and anticipate new infrastructure needs, projections and regulations.

In this work, a novel and multidisciplinary model is proposed to project vertical growth in Mexican cities. The projection is carried out with ANN techniques that work with

Table 7: Vertical urban growth model results.

Metropolitan area	Year	Skyscrapers of sample	Average accuracy	Kappa index	Jaccard index
Mexico City	2020	248	75.81%	0.7317	0.7606
	2025	339	-----	-----	-----
Guadalajara	2020	19	78.57%	0.7472	0.7723
	2025	42	-----	-----	-----
Monterrey	2020	41	73.61%	0.6866	0.7109
	2025	72	-----	-----	-----
Average	75.99%	0.7218	0.7479		

driving factors of growth in the city. Satellite image processing, vector data rasterization, neural networks and cellular automata are brought together in this work. In addition, the tool integrates with the GIS using the Python programming language, which allows for an automated model of general consultation and easy to evaluate. For urban planners who may be the most interested in using this type of tools, they can execute multiple scenarios and focus their interest on the analysis of results instead of their generation, in addition, it can be useful for government decision making.

The model has an accuracy of 75.99% regarding the projection of the number of skyscrapers, with a Kappa index of 0.7218 to evaluate the position of vertical growth and a Jaccard index of 0.7479 than in Table 6 represent good results.

Vertical growth research has areas of opportunity both with artificial intelligence and with spatial analysis techniques, so it is possible to improve the proposed model either with satellite image processing, driving factor statistics, neural network architectures or new rules of cellular automata. Future work will consist of testing the ANN and CA model in different contexts, including national satellite images and the design of new models with artificial intelligence and spatial analysis techniques, to develop public policies for the benefit of the inhabitants.

Acknowledgment

Add your acknowledgments until the acceptance of the manuscript.

References

- Abhishek N., Jenamani M., Mahanty B., (2017) Urban growth in Indian cities: Are the driving forces really changing?. *Habitat International*, 69,48-57.
- Adamatzky A., (2018). *Cellular Automata: A Volume in the Encyclopedia of Complexity and Systems Science*. Springer Publishing Company, Incorporated, EUA.
- Agatonovic-Kustrin S., Beresford R., (2000). Basic concepts of artificial neural network (ANN) modeling and its application in pharmaceutical research. *Journal of pharmaceutical and biomedical analysis*, 22(5), 717-727.
- Agyemang F., Silva E., Anokye P., (2018). Towards sustainable urban development: the social acceptability of high-rise buildings in a Ghanaian city. *GeoJournal*, 83(6), 1317-1329.
- Almeida C., Gleriani J., Castejon E., Soares-Filho B., (2008). Using neural networks and cellular automata for modelling intra-urban land-use dynamics. *International Journal of Geographical Information Science*, 22(9), 943-963.
- Anderson T., Darling D., (1954). A test of goodness of fit. *Journal of the American statistical association*, 49(268), 765-769.
- Bhatti S., Tripathi N., (2014). Built-up area extraction using Landsat 8 OLI imagery. *GIScience & remote sensing*, 51(4), 445-467.
- Bose B., (1994). Expert system, fuzzy logic, and neural network applications in power electronics and motion control. *Proceedings of the IEEE*, 82(8), 1303-1323.
- Bouchard M., Joussemle A., Doré P., (2013). A proof for the positive definiteness of the Jaccard index matrix. *International Journal of Approximate Reasoning*, 54(5), 615-626.
- Burton-Johnson A., Black M., Fretwell P., Kaluza-Gilbert J., (2016). An automated methodology for differentiating rock from snow, clous EMPORIS (2020). Locate buildings in every country around the world, 13 December 2020. <https://www.emporis.com/buildingsds> and sea in Antarctica from Landsat 8 imagery: a new rock outcrop map and area estimation for the entire Antarctic continent. *The Cryosphere*, 10(4), 1665-1677.
- CTBUH (2020). CTBUH Height criteria, 26 June 2020. <https://www.ctbuh.org>
- De Sa J., (2012). *Pattern recognition: concepts, methods and applications*, Springer Science & Business Media, Germany.
- Duque J., Lozano N., Patino J., Restrepo P., Velasquez W., (2019). Spatio-Temporal Dynamics of Urban Growth in Latin American Cities: An Analysis Using Nighttime Lights Imagery. *World Bank Policy Research Working Paper*, (8702).
- ESRI (2016). *Fundamentals of panchromatic sharpening*, 21 June 2020. <https://desktop.arcgis.com/es/arcmap/10.3/manage-data/raster-and-images/fundamentals-of-panchromatic-sharpening.htm>.
- EMPORIS (2020). Locate buildings in every country around the world, 13 December 2020. <https://www.emporis.com/buildings>
- Felix A., (2015). Impactos del crecimiento vertical en la expansión de la zona conurbada de Querétaro, Universidad Autónoma de Nuevo León.
- Gómez E., Obregón N., Rocha D., (2013). Cloud segmentation methods applied to satellite images. *Tecnura*, 17(36), 96-110.
- Haykin S., Network N., (2004). *A comprehensive foundation. Neural networks*, 2, 41.
- He Q., Liu Y., Zeng C., Chaohui Y., Tan R., (2017). Simultaneously simulate vertical and horizontal expansions of a future urban landscape: A case study in Wuhan, Central China. *International Journal of Geographical Information Science*, 31(10), 1907-1928.
- Huang Z., Lu Y., Wong N., Poh C., (2019). The true cost of “greening” a building: Life cycle cost analysis of vertical greenery systems (VGS) in tropical climate. *Journal of Cleaner Production*, 228, 437-454.
- INAFED (2015). Socioeconomic data by municipality, www.inafed.gob.mx, 18 June 2019.
- INEGI (2015a). Economically Active population, sc.inegi.org.mx/cobdem, 17 June 2019.
- INEGI (2015b). Housing, 17 June 2019. <https://www.inegi.org.mx/programas/intercensal/0A2015/default.html{\#\#}Tabulados{\%}0A>.
- INEGI (2015c). About INEGI, 17 December 2020. <https://www.inegi.org.mx/default.html>.
- INEGI (2019). Mapas geográficos, 15 December 2020. <https://www.inegi.org.mx/app/mapas/>.
- INEGI (2020). Edafología, 7 November 2020. <https://www.inegi.org.mx/temas/edafologia/>.
- Irons J., Dwyer J., Barsi J., (2012). The next Landsat satellite: The Landsat data continuity mission. *Remote Sensing of Environment*, 122, 11-21.
- Jiménez, E., Chávez, T., Garrocho, C. (2018). Modelando la expansión urbana con autómatas celulares: aplicación de la Estación de Inteligencia Territorial (Chrastaller). *Geografía y Sistemas de Información Geográfica*, Geosig, 12, 1-26.
- Jiménez E., (2019). Cadenas de Markov espaciales para simular el crecimiento del Área Metropolitana de Toluca, 2017-2031. *Economía, sociedad y territorio*, 19(60), 109-140.
- Jiménez E., (2022). Inverse Filter in the Growth of Urban Sprawl with Cellular Automata Model. In *Complex Systems and Their Applications: Second*

- International Conference (EDIESCA 2021) (pp. 231-247). Cham: Springer International Publishing.
- Kaviari F., Mesgari M., Seidi E., Motieyan H., (2019). Simulation of urban growth using agent-based modeling and game theory with different temporal resolutions. *Cities*, 95, 102387.
- Kotkar S., Jadhav B., (2015). Analysis of various change detection techniques using satellite images. In 2015 International Conference on Information Processing (ICIP), IEEE, 664-668.
- Koziatek O., Dragičević S., (2019). A local and regional spatial index for measuring three-dimensional urban compactness growth. *Environment and Planning B: Urban Analytics and City Science*, 46(1), 143-164.
- Kristollari V., Karathanassi V., (2020). Artificial neural networks for cloud masking of Sentinel-2 Ocean images with noise and sunglint. *International Journal of Remote Sensing*, 41(11), 4102-4135.
- Lampe O., Hauser H., (2011). Interactive visualization of streaming data with kernel density estimation. In 2011 IEEE pacific visualization symposium, 171-178.
- Massey F., (1951). The Kolmogorov-Smirnov test for goodness of fit. *Journal of the American statistical Association*, 46(253), 68-78.
- Montgomery D., (2017). *Design and analysis of experiments*. John Wiley & sons, EUA.
- Mualam N., Salinger E., Max D., (2019). Increasing the urban mix through vertical allocations: Public floorspace in mixed use development. *Cities*, 87, 131-141.
- Mustafa A., Cools M., Saadi I., Teller J., (2017). Coupling agent-based, cellular automata and logistic regression into a hybrid urban expansion model (HUEM). *Land Use Policy*, 69, 529-540.
- Openshaw S., Taylor P., (1984). *The modifiable unit areal problem*, Norwich: Geo books, England.
- Ou C., Yang J., Du Z., Li P., Zhu D., (2018). Simulating Multiple Land Use Changes by Incorporating Deep Belief Network into Cellular Automata: A Case Study in BEIJING-TIANJINHEBEI Region, China. *China. Lund*, 12-15.
- Palma, J., Morales, R., (2008). *Inteligencia artificial. Técnicas, métodos y aplicaciones*. Mc Graw.
- Parker M., (2014). Skyscrapers: The city and the megacity. *Theory, culture & society*, 31(7-8) 267-271.
- Rajasekaran S., Pai G.V., (2003). *Neural networks, fuzzy logic and genetic algorithm: synthesis and applications*. PHI Learning Pvt. Ltd, New Delhi.
- Richardson D., Van Oosterom P., (2002). *Advances in Spatial Data Handling: 10th International Symposium on Spatial Data Handling*. Springer Science & Business Media.
- Sabater, N., Ruiz-Verdú, A., Delegido, J., Fernández-Beltrán, R., Latorre-Carmona, P., Pla, F., ... \& Moreno, J. (2016). Development of advanced products for the SEOSAT/Ingenio mission. *Revista de Teledetección*, (47), 23-40.
- Shim J., Park S., Park E., (2004). Public space planning of mixed-use high-rise buildings—focusing on the use and impact of deck structure in an urban development in Seoul. *Tall buildings in historical cities—culture and technology for sustainable cities*, Seoul, South Korea, 13, 764-771.
- Silva E., (2004). The DNA of our regions: artificial intelligence in regional planning. *Futures*, 36(10), 1077-1094.
- SKYCRAPER (2020), Metropolitan Areas, 12 October 2020. <https://skyscraperpage.com/database/metro/>, skyscraperpage.com/database/metro/
- Tallarida R., Murray R., (1987). Chi-square test. In *Manual of pharmacologic calculations* (pp. 140-142). Springer, EUA.
- Tobler W., (1970). A computer movie simulating urban growth in the Detroit region. *Economic geography*, 46(sup1).
- USGS (2020), EarthExplorer, earthexplorer.usgs.gov, 04 April 2021.
- Wang L., Zeng Y., Chen T., (2015). Back propagation neural network with adaptive differential evolution algorithm for time series forecasting. *Expert Systems with Applications*, 42(2) 855-863.
- Wu N., Silva E., (2010). Artificial intelligence solutions for urban land dynamics: a review. *Journal of Planning Literature*, 24(3), 246-265.
- Zhang W., Li W., Zhang C., Hanink D., Liu Y., Zhai R., (2018). Analyzing horizontal and vertical urban expansions in three East Asian megacities with the SS-coMCRF model. *Landscape and urban planning*, 177, 114-127.
- Zhao C., Jensen J., Zhan B., (2017). A comparison of urban growth and their influencing factors of two border cities: Laredo in the US and Nuevo Laredo in Mexico. *Applied geography*, 79, 223-234.